

Bose-Einstein condensates and the thin-shell limit in anisotropic bubble traps

Elias J. P. Biral¹, Natália S. Móller², Axel Pelster³, F. Ednilson A. dos Santos⁴

¹ Instituto de Física de São Carlos, Universidade de São Paulo, 13560-550 São Carlos, SP, Brazil

² RCQI, Institute of Physics, Slovak Academy of Sciences, Dúbravská Cesta 9, 84511 Bratislava, Slovakia

³ Physics Department and Research Center Optimas, Technische Universität Kaiserslautern, 67663 Kaiserslautern, Germany

⁴ Department of Physics, Federal University of São Carlos, 13565-905 São Carlos, SP, Brazil

Abstract.

Within the many different models that appeared with the use of cold atoms to design BECs the bubble trap shaped potential has been of great interest. For the anisotropic bubble trap physics in the thin-shell limit the relationship between the physical parameters and the resulting manifold geometry is yet to be fully understood. In this paper, we work towards this goal showing how the parameters of the system must be manipulated in order to allow for a non-collapsing thin-shell limit. In such a limit, a dimensional compactification takes place thus leading to an effective 2D Hamiltonian which relates to up-to-date bubble trap experiments. At last, our Hamiltonian is perturbatively solved for some particular cases as applications of our theory.

1. Introduction

In the 1990's, the experimental realization of Bose-Einstein Condensates (BEC) [1, 2] gave rise to a myriad of both theoretical and experimental studies with contributions ranging from the basic understanding of the underlying physics of this interesting macroscopic quantum phenomenon to the applications in particular cases of interest. Among the vast knowledge developed, there is the creation of bubble trap physics [3–5], which consists of thin-shell traps created using a radiofrequency field in an adiabatic potential based on a quadrupolar magnetic trap.

The idea to work with two-dimensional superfluid manifolds soon proved to be appealing to physicists since the fine tune in the geometry opens new possibilities of physical interest. As a natural consequence, many experiments appeared in the literature [6–10]. Unfortunately, there are various technical difficulties in creating bubble trap experiments among which is the gravitational sag, i.e., the sinking of the BEC atoms into the bottom of the trap. With the current developments, it is possible to escape this problem working with microgravity either with free-falling experiments on earth-based laboratories [11, 12] or space-based in the International Space Station with the Cold Atom Laboratory (CAL) [13–19]. Up until today, the usual microgravity [20] seems to be the best solution for confining atomic gases into shells in order to study its properties, but some new alternatives such as gravity compensation mechanisms are arising [21, 22]. Also, an interesting substitute to the usual procedure of

radio-frequency dressing was proposed working with dual-species atomic mixture [23], which led to the creation of a BEC on Earth's gravity [24].

Confinements in three-dimensional shell shaped condensates inspired some theoretical works worth mentioning here. In [25], the authors apply both analytical and numerical techniques in order to investigate the ground state wave function of a BEC, its collective modes, and some expansion properties. The interesting paper [26] employs thermodynamic arguments in order to survey clusters formations. The thermodynamics of a BEC on a spherical shell is analyzed, including the critical temperature in [27–29]. The topological hollowing transition from a full sphere to a thin-shell was studied in [30] and [31], thus finding some universal properties. The ground state and collective excitations of a dipolar BEC was considered in [32]. The general physical relevance of cold atoms on curved manifolds is also addressed in [33]. The contribution of [34] plays with the idea that the external potential is equivalent to the harmonic trap for a large radius thin-shell. Universal scaling relations are found for topological superfluid transitions in bubble traps in [35]. Non-Hermitian phase transitions are meticulously described in [36]. Although it is not the focus of this work, it is also worth citing vortex studies on spherical-like surfaces with no holes [37–44].

This paper aims to explain the relationship between the geometrical distortion of a bubble trap, its curvature, and the confinement of the particles in the thin-shell limit. Section 2 describes the mathematical background applied in our work defining the concepts and explaining the theoretical basis in which our theory is developed. In section 3, the second step towards the building of our theoretical development is made by calculating the harmonic radial frequency in the Gaussian-Normal coordinate system (GNCS) where its angular dependency is exposed, the definition of the thin-shell limit is discussed in a rigorous mathematical way showing its dependence on the bubble trap geometrical distortion, and also, a particular application of our theory is shown. The general Gross-Pitaevskii Hamiltonian of the system is deduced using a perturbative approach near the thin-shell limit in section 4. In section 5, special topics of the spherical shell and the Thomas-Fermi approximation are considered. Finally, in section 6, the corresponding effective Gross-Pitaevskii equation is perturbatively solved for small distortions in order to determine both the ground-state wavefunction and the oscillation frequencies.

2. Gaussian Normal Coordinate System

In this section, some preliminary concepts that are important to our work are defined and explained in order to establish the theoretical background in which our theory is developed. One of the main concepts, that are important to be defined, concerns the manifold [45, 46] considered here. In this work, we use 2D surfaces embedded into a 3D Euclidean space. More specifically, ellipsoidal surfaces [47–49] are considered since they correspond to the bubble trap potentials in BEC experiments. Therefore, our manifolds are compact, smooth and differentiable everywhere.

In this work we choose a suitable coordinate system to describe the 3D region around our 2D manifold: the so-called Gaussian Normal Coordinate System (GNCS) [50, 51]. Further features and particularities on its application can be found by the interested reader in [52].

It is always possible to describe the region around smooth manifolds with the aid of a GNCS. The main idea to understand is that our 2D manifold M has two coordinates x^1 and x^2 , also called tangent coordinates, describing arbitrary points in the manifold. Thus, any point \mathbf{p} of this manifold M is portrayed by the position vector $\vec{p}(x^1, x^2)$. Any point \mathbf{q} in such a vicinity of M can be represented with the aid of the coordinate x^0 referred to as the orthogonal coordinate, and a normal unit vector \hat{n} at the point \mathbf{p} through the following equation

$$\vec{q}(x^0, x^1, x^2) = \vec{p}(x^1, x^2) + x^0 \hat{n}(x^1, x^2). \quad (1)$$

We define the geometrical shape of the manifold in question with the aid of the prolate spheroidal coordinates [53, 54]. The transformation equations between such a system of coordinates and the

Cartesian system allows us to establish the following family of ellipsoidal surfaces

$$\begin{cases} x = A \sin \nu \cos \phi \\ y = A \sin \nu \sin \phi \\ z = \frac{A}{\sqrt{1+\epsilon}} \cos \nu \end{cases}, \begin{cases} \phi \in [0, 2\pi) \\ \nu \in [0, \pi) \\ A \in [0, \infty) \end{cases} \quad (2)$$

with $\nu = x^1$ and $\phi = x^2$ being the tangent coordinates, the parameter ϵ the geometrical distortion between an ellipsoid and a sphere according to the equation $x^2 + y^2 + (1 + \epsilon)z^2 = A^2$, where A is a quantity analogous to a sphere radius which determines the overall size of the ellipsoid.

For each point on the manifold M it is possible to determine a pair of mutually orthogonal vectors tangent to the manifold by taking partial derivatives of $\vec{p}(\nu, \phi)$

$$\begin{cases} \vec{v}_1(\nu, \phi) = \frac{\partial \vec{p}(\nu, \phi)}{\partial \nu} = A \cos \nu \cos \phi \hat{x} + A \cos \nu \sin \phi \hat{y} - \frac{A}{\sqrt{1+\epsilon}} \sin \nu \hat{z}, \\ \vec{v}_2(\nu, \phi) = \frac{\partial \vec{p}(\nu, \phi)}{\partial \phi} = -A \sin \nu \sin \phi \hat{x} + A \sin \nu \cos \phi \hat{y}. \end{cases} \quad (3)$$

This way, the unitary normal vector can be written as

$$\hat{n} = \frac{\frac{\partial \vec{p}(\nu, \phi)}{\partial \nu} \times \frac{\partial \vec{p}(\nu, \phi)}{\partial \phi}}{\left| \frac{\partial \vec{p}(\nu, \phi)}{\partial \nu} \times \frac{\partial \vec{p}(\nu, \phi)}{\partial \phi} \right|} = \frac{\sin \nu \cos \phi \hat{x} + \sin \nu \sin \phi \hat{y} + \sqrt{1+\epsilon} \cos \nu \hat{z}}{\sqrt{1 + \epsilon \cos^2 \nu}}. \quad (4)$$

These vectors form an orthogonal basis according to the following properties

$$\hat{n} \cdot \hat{n} = 1, \quad \vec{v}_1 \cdot \hat{n} = 0, \quad \vec{v}_2 \cdot \hat{n} = 0, \quad \vec{v}_1 \cdot \vec{v}_2 = 0. \quad (5)$$

Choosing $x^0 = s$, the set of coordinates $(x^0, x^1, x^2) = (s, \nu, \phi)$ define our GNCS.

The visualization of the coordinates and vectors outlined in this section is exposed in figure 1. There, it is shown a drawing of the manifold M as an ellipsoid including the GNCS. The vector $\vec{p}(\nu, \phi)$ points to the point \mathbf{p} at the manifold, where $s = 0$. The two tangent vectors $\vec{v}_1(\nu, \phi)$ and $\vec{v}_2(\nu, \phi)$, and the unit normal vector $\hat{n}(\nu, \phi)$ to the manifold at the point \mathbf{p} are also illustrated.

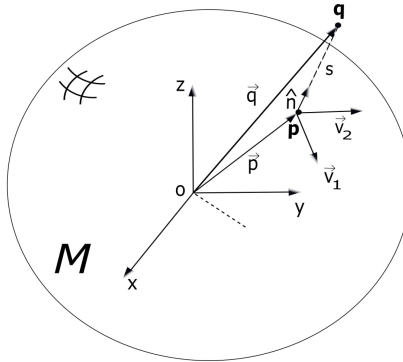


Figure 1. Drawing of the manifold M as an ellipsoid including the GNCS with $(x^0, x^1, x^2) = (s, \nu, \phi)$ described with the aid of the prolate spheroidal coordinates developed in this section.

With this mathematical background, let us write the metric tensor [55] of the system as $G_{\alpha\beta} = \frac{\partial \vec{q}(s, \nu, \phi)}{\partial x^\alpha} \cdot \frac{\partial \vec{q}(s, \nu, \phi)}{\partial x^\beta}$, which, in matrix notation according to the properties (5) has the typical form of GNCS

$$G_{\alpha\beta} = \begin{bmatrix} 1 & 0 & 0 \\ 0 & \left(\cos^2 \nu + \frac{\sin^2 \nu}{1+\epsilon} \right) \left(A + s \frac{1+\epsilon}{(1+\epsilon \cos^2 \nu)^{3/2}} \right)^2 & 0 \\ 0 & 0 & \sin^2 \nu \left(A + s \frac{1}{\sqrt{1+\epsilon \cos^2 \nu}} \right)^2 \end{bmatrix}. \quad (6)$$

It is important to realize that in the case of a spherical shell, with $\epsilon = 0$, we recover the result of the metric tensor for spherical coordinates [56] where $r = A + s$ is the radial coordinate and the polar angle is ν .

3. Thin-shell limit for bubble traps

In this section, let us explain which potentials this work deals with. We consider a 3D potential which is both constant and has its lowest value along the manifold M . Later we show how such conditions are consistent with actual experimental potentials.

3.1. Confinement potential in a bubble trap

In order to make the reading easier, the notation is simplified according to $(x^0, x^1, x^2) \equiv (s, x^i)$.

The initial idea is to write our general potential as

$$V(s, x^i) = \Lambda^2 v(s, x^i), \quad (7)$$

where the parameter Λ controls the strength of the confinement with the limit $\Lambda \rightarrow \infty$ corresponding to a infinitely tight potential thus defining the thin-shell limit. In addition, the factor $v(s, x^i)$ must be chosen in such a way that it fulfills the requisites of being a constant at the surface of the manifold M and having a vanishing first derivative with respect to s for $s = 0$. In this section, additional considerations on the definition of the thin-shell limit relating it to the geometrical distortion of the shell will be exposed.

In order to study the vicinity of the manifold M , let us start with a Taylor expansion for the orthogonal direction

$$v(s, x^i) = K + \frac{1}{2!} s^2 \frac{\partial^2 v(s, x^i)}{\partial s^2} \Big|_M + O(s^3), \quad (8)$$

with $K = v|_M$ being a constant at the minimum M , which is characterized by $s = 0$, and the first derivative in s vanishes there.

The second derivative of the potential, in the case of the bubble trap, defines the harmonic frequency $\Lambda\Omega$ around the vicinity of the shell. This derivative is

$$\frac{\partial^2 v(s, x^i)}{\partial s^2} \Big|_M = \sum_{\alpha, \beta=1}^3 \frac{\partial^2 v(x, y, z)}{\partial r^\alpha \partial r^\beta} \Big|_M n^\alpha n^\beta = \hat{n} \cdot (\nabla \nabla v(x, y, z)|_M) \cdot \hat{n} = m\Omega^2(x, y, z), \quad (9)$$

where $r^1 = x$, $r^2 = y$, and $r^3 = z$ are the Cartesian coordinates, and n^α and n^β are the respective components of the normal vector.

In order to fit the usual bubble trap geometry experiments [4–9, 11–19], let us consider the finite factor of our potential in a generalized form as

$$v(x, y, z) \equiv f(x^2 + y^2 + (1 + \epsilon)z^2). \quad (10)$$

In this case the geometry of the potential is well established to be an ellipsoidal surface, which becomes spherical for $\epsilon = 0$. Thus, our manifold M is characterized by $x^2 + y^2 + (1 + \epsilon)z^2 = A^2 \Rightarrow f(x^2 + y^2 + (1 + \epsilon)z^2)|_M = f(A^2) = \text{constant}$, and $f'(A^2) = 0$.

With such a general form, let us explicitly calculate $m\Omega^2(s, x^i)$. The derivatives can be written in vector form as $\nabla v(x, y, z)|_M \cdot \hat{n} = (f'(x^2 + y^2 + (1 + \epsilon)z^2)(2x\hat{x} + 2y\hat{y} + 2(1 + \epsilon)z\hat{z}))|_M \cdot \hat{n}$. Writing \hat{n} in Cartesian coordinates, it is possible to express $\nabla v(x, y, z)|_M \cdot \hat{n} = 2f'(A^2)\sqrt{x^2 + y^2 + (1 + \epsilon)^2z^2} = 0$. Working on the second derivatives as well we read off from (9) that $m\Omega^2(x, y, z) = 4f''(A^2)(A^2 + \epsilon(1 + \epsilon)z^2)$, which becomes in terms of our GNCS

$$m\Omega^2(x^i) = 4f''(A^2)A^2(1 + \epsilon \cos^2 \nu). \quad (11)$$

This gives the final form for the harmonic frequency considering our generalized potential in an ellipsoidal surface with the appropriate constraints.

Now, some careful considerations must be made for the thin-shell limit in the case of ellipsoidal potentials.

For infinitely tight potentials, we know in advance, that the motion of particles along the normal direction is restricted to the ground state of an harmonic oscillator with frequency $\Lambda\Omega(x^i)$ which is described by a Gaussian wave function with width $\alpha = \sqrt{\hbar/m\Lambda\Omega}$. In previous works, mainly devoted to the spherical case, some authors defined the thin-shell limit as a rather generic situation, where the radius R of the sphere-shaped trap is much larger than the thickness of the shell, i.e., $\lim_{R \rightarrow \infty} \frac{R}{\alpha}$. Since these are not the only length scales in this system, different results can be obtained by either considering $R \rightarrow \infty$ or $\alpha \rightarrow 0$. For example in [44] the authors considered the situation where $R \rightarrow \infty$. In the numerical work [28] the authors made some qualitative comparisons between α and R . In some papers [30–32], the ratio R/α is chosen to be as high as possible without more detailed considerations. Our objective in this paper is to consider the specific case $\alpha \rightarrow 0$, i.e., the case where α is much smaller than any other length scale in the system. We believe that this constitutes a more rigorous definition of a thin-shell limit. Such a limit is equivalent to consider $\Lambda \rightarrow \infty$.

As already mentioned, in the thin-shell limit we expect the motion in the normal direction to be confined to the ground state of a harmonic oscillator with frequency $\Lambda\Omega$. Since for the ellipsoidal case, Ω is space dependent, every particle in the system will experience a site-dependent energy due to its confinement. Such an energy is provided by the ground-state energy of a harmonic oscillator with frequency $\Lambda\Omega$, i.e.,

$$E = \frac{\hbar\Lambda\Omega}{2} = \frac{\hbar\Lambda}{2} \sqrt{\frac{4f''(A^2)A^2(1 + \epsilon \cos^2 \nu)}{m}}. \quad (12)$$

Here we see that for $\epsilon \rightarrow 0$ this energy diverges for $\Lambda \rightarrow \infty$ thus adding a uniform infinite potential which does not have any consequence for the dynamics of the particle moving in the manifold. However for $\epsilon \neq 0$ the situation changes considerably since the particles would be subjected to an infinite space-dependent potential. Let us for example consider the energy difference between the poles and the equator $E_{\text{comp}} = E(\nu = 0) - E(\nu = \pi/2)$, and we can find that $E_{\text{comp}} \propto \Lambda$ for any non-vanishing ϵ , which means that it diverges in the thin-shell limit. This would then induce a complete localization of particles at the poles or at the equator, depending on the sign of ϵ . Thus in order to restrict our limit to physically acceptable situations, we must consider only the case of small geometrical distortions

$$\epsilon = \Lambda^{-1}\bar{\epsilon}, \quad (13)$$

where $\bar{\epsilon}$ is considered to be finite.

By taking into account (13), the induced energy difference then becomes

$$E_{\text{comp}} = \frac{\hbar}{4} \sqrt{\frac{4f''(A^2)A^2}{m}} \bar{\epsilon} + O(\Lambda^{-1}), \quad (14)$$

which is finite in the thin-shell limit.

For arbitrary values of ν , Eq. (12) becomes

$$E = \frac{\hbar\Lambda}{2} \sqrt{\frac{4f''(A^2)A^2}{m}} + \bar{\epsilon} \frac{\hbar}{4} \sqrt{\frac{4f''(A^2)A^2}{m}} \cos^2 \nu + O(\Lambda^{-1}). \quad (15)$$

From (15), we see that the energy per particle generated due to the compactification process separates into one infinite site-independent part and a finite site-dependent part. It means that, in the thin-shell limit, each particle is effectively subjected to a compactification potential given by

$$V_{\text{comp}} = \bar{\epsilon} \frac{\hbar}{4} \sqrt{\frac{4f''(A^2)A^2}{m}} \cos^2 \nu. \quad (16)$$

In experimental terms, the infinitesimal eccentricity $\epsilon = \Lambda^{-1}\bar{\epsilon}$ corresponds to the situation where the difference between the larger axis and the smaller axis of the ellipsoid is of the same order of the Gaussian width α . This means that in order to avoid the particle collapse to either the poles or the equator, the ellipsoidal eccentricity must be kept within such bounds.

In the next subsections, let us consider an experimental realization of the general potential (10) as a generic example where our theory can be realized.

3.2. Confinement potential in experiments

In this subsection, we apply the calculations to a particular confinement potential. There are some variations of this potential in the literature that differ in the way the potential is defined, for instance, by including gravity effects or considering frequency anisotropy [4, 5].

Here let us consider the more concrete experimental example in [6] to the application of our theory, where

$$V_{\text{E}}(x, y, z) = \sqrt{(V_{\text{trap}}(x, y, z) - \hbar\Delta)^2 + (\hbar\Omega_{\text{RF}})^2}, \quad (17)$$

with $V_{\text{trap}}(x, y, z) = \omega^2 v_{\text{trap}}(x, y, z) = \frac{m\omega^2}{2}(x^2 + y^2 + (1 + \epsilon)z^2)$. Here $\hbar\Delta = \hbar\omega_{\text{rf}} - V_0$ denotes the rf detuning with respect to the rf transition in the center of the magnetic trap, and $\Omega_{\text{RF}} = \frac{g\mu_{\text{B}}B_1}{2\hbar}$ stands for the Rabi frequency of the magnetic field $B_1 \cos(\omega_{\text{rf}}t)$ where $g = 1/2$ and μ_{B} is the Bohr magneton, and ϵ represents the geometrical distortion of the ellipsoid. This potential has a local minimum if $V_{\text{trap}}(x, y, z) = \hbar\Delta$ for the state $F = 2$, $m_{\text{F}} = 2$.

Let us express the potential as our theory demands, i.e.,

$$V_{\text{E}}(x, y, z) = \omega^2 \sqrt{\left(v_{\text{trap}}(x, y, z) - \frac{\hbar\Delta}{\omega^2}\right)^2 + \left(\frac{\hbar\Omega_{\text{RF}}}{\omega^2}\right)^2} = \omega^2 v_{\text{E}}(x, y, z), \quad (18)$$

which defines a function f according to (10), where Λ^2 equals to ω^2 in this particular case.

The thin-shell limit for such a potential can be obtained by considering $\omega \rightarrow \infty$, $\Delta \rightarrow \infty$, and $\Omega_{\text{RF}} \rightarrow \infty$ while the radius $\frac{\hbar\Delta}{\omega^2}$ and $\frac{\hbar\Omega_{\text{RF}}}{\omega^2}$ are kept finite. Also $\epsilon\omega$ must be kept finite in order to prevent the collapse of the condensate.

The expression for the harmonic frequency (11) with our GNCS and $A = \sqrt{\frac{2\hbar\Delta}{m\omega^2}}$ is

$$m\Omega_{\text{E}}^2(x^i) = \frac{2m\Delta}{\Omega_{\text{RF}}} (1 + \epsilon \cos^2 \nu). \quad (19)$$

In more experimental terms, the range of parameters corresponding to the thin-shell limit occur when $\alpha \ll A$, which corresponds to

$$\frac{2\Delta}{\omega} \gg \sqrt{\frac{\Omega_{\text{RF}}}{2\Delta}}, \quad (20)$$

while in order to prevent the collapse of the condensate, we must also have $\epsilon A \sim \alpha$, i. e.,

$$\epsilon^2 \sim \frac{\omega}{2\Delta} \sqrt{\frac{\Omega_{\text{RF}}}{2\Delta}}. \quad (21)$$

Within the thin-shell limit for this particular experimental case of our theory, equation (7) with the aid of (8) becomes

$$V_{\text{E}}(s, x^i) = \omega^2 \left(\frac{\hbar\Omega_{\text{RF}}}{\omega^2} + \frac{1}{2!} s^2 \frac{2m\Delta}{\Omega_{\text{RF}}} (1 + \omega^{-1} \bar{\epsilon} \cos^2 \nu) + O(s^3) \right). \quad (22)$$

And the corresponding compactification potential follows from Eq. (16)

$$V_{\text{comp}} = \bar{\epsilon} \frac{\hbar}{4} \sqrt{\frac{2\Delta}{\Omega_{\text{RF}}}} \cos^2 \nu. \quad (23)$$

Such expressions confirm that the general theory presented here is well suited to deal with the already created experimental bubble-trap potentials.

4. Effective Hamiltonian in the thin-shell limit

In this section, we will consider the thin-shell limit for interacting particles. Let us begin with the usual Gross-Pitaevskii Hamiltonian

$$H = \int d^3x \left\{ \frac{\hbar^2}{2m} |\nabla \Psi|^2 + V(x, y, z) |\Psi|^2 + \frac{g_{\text{int}}}{2} |\Psi|^4 \right\}, \quad (24)$$

written in Cartesian coordinates, where m defines the mass of the particles, V stands for the overall potential and g_{int} represents the interaction parameter. The total number of particles is given by

$$N = \int d^3x \Psi^* \Psi. \quad (25)$$

Rewriting the Hamiltonian in our GNCS yields approximately

$$H \approx \int dx^i \int_{s^-(u)}^{s^+(u)} ds \sqrt{|g|} \left\{ -\frac{\hbar^2}{2m} \Psi^* \left[|g|^{-1/2} \frac{\partial}{\partial s} \left(|g|^{1/2} \frac{\partial \Psi}{\partial s} \right) + |g|^{-1/2} \frac{\partial}{\partial x^i} \left(|g|^{1/2} g^{ij} \frac{\partial \Psi}{\partial x^j} \right) \right] \right. \\ \left. + V(s, x^i) \Psi^* \Psi + \frac{g_{\text{int}}}{2} \Psi^* \Psi^2 \right\}, \quad (26)$$

where g is the reduced metric

$$g_{ij} = \begin{bmatrix} \left(\cos^2 \nu + \frac{\sin^2 \nu}{1+\epsilon} \right) \left(A + s \frac{1+\epsilon}{(1+\epsilon \cos^2 \nu)^{3/2}} \right)^2 & 0 \\ 0 & \sin^2 \nu \left(A + s \frac{1}{\sqrt{1+\epsilon \cos^2 \nu}} \right)^2 \end{bmatrix}, \quad (27)$$

which has only the elements corresponding to the tangent coordinates. The limits of the s integral are chosen in such a way that both $(\Lambda \Omega m s^{-2})/\hbar \gg 1$ and $(\Lambda \Omega m s^{+2})/\hbar \gg 1$. This assures that the difference between (24) and (26) decays exponentially for $\Lambda \rightarrow \infty$ since $\Psi \sim e^{-(\Lambda \Omega(u) m s^2)/2\hbar}$ in the thin-shell limit.

In order to simplify our calculations, we follow [52] and consider the alternative wave function $\tilde{\Psi}$

$$\Psi(s, x^i) = \frac{|g_0(x^i)|^{1/4}}{|g(s, x^i, \epsilon)|^{1/4}} \tilde{\Psi}(s, x^i), \quad (28)$$

where $g_0(x^i) = g(0, x^i, 0)$. Note that the normalization condition 25 for $\tilde{\Psi}$ then becomes

$$N \approx \int dx^i \sqrt{|g_0|} \int_{s^-(u)}^{s^+(u)} ds \tilde{\Psi}^* \tilde{\Psi}. \quad (29)$$

This allows us to use the 2D s -independent Jacobian $\sqrt{|g_0|}$ also for the Hamiltonian, as follows

$$\begin{aligned} H \approx & \int dx^i \sqrt{|g_0|} \int_{s^-(u)}^{s^+(u)} ds \left\{ -\frac{\hbar^2}{2m} \frac{|g|^{1/4}}{|g_0|^{1/4}} \tilde{\Psi}^* \left[|g|^{-1/2} \frac{\partial}{\partial s} \left(|g|^{1/2} \frac{\partial}{\partial s} \left(\frac{|g_0|^{1/4}}{|g|^{1/4}} \tilde{\Psi} \right) \right) \right] \right. \\ & \left. + |g|^{-1/2} \frac{\partial}{\partial x^i} \left(|g|^{1/2} g^{ij} \frac{\partial}{\partial x^j} \left(\frac{|g_0|^{1/4}}{|g|^{1/4}} \tilde{\Psi} \right) \right) \right] + V(s, x^i, \epsilon) \tilde{\Psi}^* \tilde{\Psi} + \frac{g_{\text{int}}}{2} \frac{|g_0|^{1/2}}{|g|^{1/2}} \tilde{\Psi}^{*2} \tilde{\Psi}^2 \right\}. \end{aligned} \quad (30)$$

Defining $\gamma(s, \epsilon) \equiv \frac{|g|}{|g_0|}$, it is possible to rewrite our Hamiltonian as

$$\begin{aligned} H \approx & \int dx^i \sqrt{|g_0|} \int_{s^-(u)}^{s^+(u)} ds \left\{ -\frac{\hbar^2}{2m} \gamma^{-1/4} \tilde{\Psi}^* \frac{\partial}{\partial s} \left(\gamma^{1/2} \frac{\partial}{\partial s} \left(\gamma^{-1/4} \tilde{\Psi} \right) \right) \right. \\ & - \frac{\hbar^2}{2m} |g_0|^{-1/2} \gamma^{-1/4} \tilde{\Psi}^* \frac{\partial}{\partial x^i} \left(|g_0|^{1/2} \gamma^{1/2} g^{ij} \frac{\partial}{\partial x^j} \left(\gamma^{-1/4} \tilde{\Psi} \right) \right) \\ & \left. + V(s, x^i, \epsilon) \tilde{\Psi}^* \tilde{\Psi} + \frac{g_{\text{int}}}{2} \gamma^{-1/2} \tilde{\Psi}^{*2} \tilde{\Psi}^2 \right\}. \end{aligned} \quad (31)$$

As already mentioned, in the thin-shell limit we expect $\tilde{\Psi} \sim e^{-(\Lambda \Omega m s^2)/2\hbar}$, i.e., $\tilde{\Psi}$ depends implicitly on Λ . In order to make such a dependency explicit while maintaining the normalization of $\tilde{\Psi}$ as well as to keep the interaction term finite in the limit $\Lambda \rightarrow \infty$, we perform the following scale transformations

$$\begin{cases} s = \Lambda^{-1/2} y, \\ \tilde{\Psi} = \Lambda^{1/4} \psi; \quad \tilde{\Psi}^* = \Lambda^{1/4} \psi^*, \\ g_{\text{int}} = \Lambda^{-1/2} \bar{g}_{\text{int}}, \end{cases} \quad (32)$$

that gives us some extra control over the Taylor expansions to be performed inside the integrals. These rescaled quantities are the normal direction s , the wave function $\tilde{\Psi}$, and the particle interaction g_{int} .

With the abbreviations $\gamma_1 = \partial\gamma/\partial s$, $\gamma_2 = \partial^2\gamma/\partial s^2$, we can make the substitution $\gamma^{-1/4} \frac{\partial}{\partial s} \left(\gamma^{1/2} \frac{\partial}{\partial s} \left(\gamma^{-1/4} \tilde{\Psi} \right) \right) = \frac{\partial^2 \tilde{\Psi}}{\partial s^2} + \left(\frac{3}{16} \frac{\gamma_1^2}{\gamma^2} - \frac{1}{4} \frac{\gamma_2}{\gamma} \right) \tilde{\Psi}$. This identity together with (7) and (32) give us the Hamiltonian

$$\begin{aligned} H \approx \int dx^i \sqrt{|g_0|} \int_{\Lambda^{1/2}s^-(u)}^{\Lambda^{1/2}s^+(u)} dy \Big\{ & -\Lambda \frac{\hbar^2}{2m} \psi^* \frac{\partial^2 \psi}{\partial y^2} - \frac{\hbar^2}{2m} \left(\frac{3}{16} \frac{\gamma_1^2}{\gamma^2} - \frac{1}{4} \frac{\gamma_2}{\gamma} \right) \psi^* \psi \\ & - \frac{\hbar^2}{2m} \gamma^{-1/4} \psi^* |g_0|^{-1/2} \frac{\partial}{\partial x^i} \left(|g_0|^{1/2} \gamma^{1/2} g^{ij} \frac{\partial}{\partial x^j} \left(\gamma^{-1/4} \psi \right) \right) \\ & + \Lambda^2 v(\Lambda^{-1/2} y, x^i, \Lambda^{-1} \epsilon) \psi^* \psi + \frac{\bar{g}_{\text{int}}}{2} \gamma^{-1/2} \psi^{*2} \psi^2 \Big\}, \end{aligned} \quad (33)$$

Now we can expand both v and γ in a power series with respect to $\Lambda^{-1/2}$ which gives us

$$\begin{aligned} \Lambda^2 v(\Lambda^{-1/2} y, x^i, \Lambda^{-1} \epsilon) &= \Lambda^2 K + \Lambda \frac{1}{2} 4f''(A^2) A^2 y^2 \\ &+ \Lambda^{1/2} \frac{1}{6} (8f'''(A^2) A^3 + 12f''(A^2) A) y^3 + \frac{\bar{\epsilon}}{2} 4f''(A^2) A^2 \cos^2 \nu y^2 \\ &+ \frac{1}{24} (16f^{IV}(A^2) A^4 + 48f'''(A^2) A^2 + 12f''(A^2)) y^4 + O(\Lambda^{-1/2}). \end{aligned} \quad (34)$$

Note that we have

$$\gamma = 1 + O(\Lambda^{-1/2}), \quad (35)$$

and according to Appendix A we conclude that

$$\left(\frac{3}{16} \frac{\gamma_1^2}{\gamma^2} - \frac{1}{4} \frac{\gamma_2}{\gamma} \right) = O(\Lambda^{-1/2}). \quad (36)$$

Observe that the presence of the harmonic frequency in (11) considering (13) leads to $m\Omega^2 = 4f''(A^2) A^2 + \Lambda^{-1} \bar{\epsilon} 4f''(A^2) A^2 \cos^2 \nu = m\Omega_0^2 + \Lambda^{-1} \bar{\epsilon} m\Omega_0^2 \cos^2 \nu$, where

$$m\Omega_0^2 = 4f''(A^2) A^2. \quad (37)$$

Substituting these equations and neglecting exponentially decaying contributions, the Hamiltonian can be written as $H = H_2 + H_1 + H_{1/2} + H_0 + O(\Lambda^{-1/2})$, where the respective terms are sorted according decreasing contributions

$$H_2 = \Lambda^2 K \int dx^i \int dy \sqrt{|g_0|} \psi^* \psi = \Lambda^2 K N = E_2, \quad (38)$$

$$H_1 = \Lambda \int dx^i \int dy \sqrt{|g_0|} \left\{ -\frac{\hbar^2}{2m} \psi^* \frac{\partial^2 \psi}{\partial y^2} + \frac{1}{2} m\Omega_0^2 y^2 \psi^* \psi \right\}, \quad (39)$$

$$H_{1/2} = \Lambda^{1/2} \int dx^i \int dy \sqrt{|g_0|} \left\{ \left(\frac{1}{6} (8f'''(A^2) A^3 + 12f''(A^2) A) y^3 \right) \psi^* \psi \right\}, \quad (40)$$

$$\begin{aligned} H_0 &= \int dx^i \int dy \sqrt{|g_0|} \left\{ -\frac{\hbar^2}{2m} \psi^* |g_0|^{-1/2} \frac{\partial}{\partial x^i} \left(|g_0|^{1/2} g_0^{ij} \frac{\partial}{\partial x^j} \psi \right) \right. \\ &+ \frac{\bar{\epsilon}}{2} m\Omega_0^2 y^2 \cos^2 \nu \psi^* \psi \\ &\left. + \frac{1}{24} (16f^{IV}(A^2) A^4 + 48f'''(A^2) A^2 + 12f''(A^2)) y^4 \psi^* \psi + \frac{\bar{g}_{\text{int}}}{2} \psi^{*2} \psi^2 \right\}, \end{aligned} \quad (41)$$

with limits for the integrals in y being $-\infty$ to ∞ . Since H_2 is a simple additive constant, our analysis effectively starts with H_1 .

Note that H_1 lacks an interaction term and essentially corresponds to the harmonic oscillator Hamiltonian whose spectrum is given by the linear eigenvalue equation

$$-\frac{\hbar^2}{2m} \frac{\partial^2 \psi}{\partial y^2} + \frac{1}{2} m \Omega_0^2 y^2 \psi = \frac{E_1}{\Lambda} \psi. \quad (42)$$

At order Λ_0 the degenerate eigenfunctions of 42 are given by

$$\begin{aligned} \psi_{n,l}^{(0)}(y, x^i) &= \psi_{n\perp}(y) \xi_l(x^i) \\ &= \frac{1}{\sqrt{2^n n!}} \left(\frac{m \Omega_0}{\pi \hbar} \right)^{1/4} \exp \left(-\frac{m \Omega_0}{2 \hbar} y^2 \right) H_n \left(\sqrt{\frac{m \Omega_0}{\hbar}} y \right) \xi_l(x^i), \end{aligned} \quad (43)$$

where H_n are the Hermite polynomials, $\psi_{n\perp}$ are the harmonic oscillator eigenstates, and ξ_l arbitrary functions of x^i obeying the condition $\sum_l \int dx^i \sqrt{|g_0|} \xi_l^*(x^i) \xi_l(x^i) = N$. The dominant contribution to the energy spectrum of system reads

$$E_n^{(1)} = N \Lambda \hbar \Omega_0 \left(\frac{1}{2} + n \right). \quad (44)$$

Therefore, in the thin-shell limit where $\Lambda \rightarrow \infty$, the system acquires finitely separated energy bands. This implies that, physically, only the lowest energy band with energy $E_1 = E_0^{(1)} = N \Lambda \hbar \Omega_0 / 2$ will be populated with particles, i.e., $\xi_l^* = 0$ for $l \neq 0$. In particular, the normalization condition for ξ_0 becomes

$$\int dx^i \sqrt{|g_0|} \xi_0^*(x^i) \xi_0(x^i) = N. \quad (45)$$

Now, let us deal with the effects of the $H_{1/2}$ contribution to the total Hamiltonian. Similar to H_1 , also $H_{1/2}$ acts only in the subspace defined by the variable y . This means that it will induce corrections of order $\Lambda^{-1/2}$ to $\psi_{n\perp}$ as well as corrections of order $\Lambda^{1/2}$ to the energies (44). Such corrections of order $\Lambda^{-1/2}$ to $\psi_{n\perp}$ can be neglected at the thin-shell limit while the contribution with power $\Lambda^{1/2}$ to (44) vanishes according to

$$E_n^{(1/2)} = \Lambda^{1/2} \int dx^i \int_{-\infty}^{+\infty} dy \sqrt{|g_0|} \left\{ \left(\frac{1}{6} (8 f'''(A^2) A^3 + 12 f''(A^2) A) y^3 \right) \psi_{n,0}^{*(0)} \psi_{n,0}^{(0)} \right\} = 0. \quad (46)$$

Although the contribution to energy with power $\Lambda^{1/2}$ vanishes, an application of second-order perturbation theory considering $H_{1/2}$ as a perturbation over H_1 shows that contributions with power Λ^0 to (44) do not vanish. In particular the correction $E_0^{(0)}$ to $E_0^{(1)}$ due to $H_{1/2}$ is

$$E_0^{(0)} = -\frac{11 N \hbar^2}{18 m} \left(\frac{2 f'''(A^2) A^3 + 3 f''(A^2) A}{4 f''(A^2) A^2} \right)^2. \quad (47)$$

Further contributions to (44) due to $H_{1/2}$ are of order $\Lambda^{-1/2}$ and are negligible in the thin-shell limit.

Finally we must consider the effect of H_0 over the energy spectrum and eigenstates. The first thing to observe is that H_0 also acts over the subspace defined by the coordinates x^i , which implies

that H_0 is able to break the degeneracy. Therefore at order Λ^0 the system is effectively separated into disjoint subspaces, each one having wave functions given by $\psi_{n\perp}(y)\xi_n(x^i)$. According to (44), the energy gap between such subspaces is of the order of Λ , which means that in the thin-shell limit where $\Lambda \rightarrow \infty$ only the subspace with lowest energy becomes occupied. Therefore the systems wave function in the thin-shell limit must be

$$\psi(y, x^i) = \left(\frac{m\Omega_0}{\pi\hbar} \right)^{1/4} \exp \left(-\frac{m\Omega_0}{2\hbar} y^2 \right) \xi(x^i), \quad (48)$$

where $\xi(x^i) = \xi_0(x^i)$. Substituting (48) into H_0 and integrating where possible yields the constant contribution

$$C_0 = \frac{N}{8} \frac{\hbar^2}{m} \left(\frac{4f^{IV}(A^2)A^4 + 12f'''(A^2)A^2 + 3f''(A^2)}{4f''(A^2)A^2} \right) \quad (49)$$

in addition to the effective Hamiltonian

$$H_{\text{eff}} = \int dx^i \sqrt{|g_0|} \left\{ -\frac{\hbar^2}{2m} \xi^* |g_0|^{-1/2} \frac{\partial}{\partial x^i} \left(|g_0|^{1/2} g_0^{ij} \frac{\partial}{\partial x^j} \xi \right) + \frac{\bar{\epsilon}}{4} \hbar \Omega_0 \cos^2 \nu \xi^* \xi + \frac{\bar{g}_{2D}}{2} \xi^{*2} \xi^2 \right\}, \quad (50)$$

which can be simplified to

$$H_{\text{eff}} = \int_0^\pi d\nu \int_0^{2\pi} d\phi A^2 \sin \nu \left\{ -\frac{\hbar^2}{2mA^2 \sin \nu} \xi^* \left[\frac{\partial}{\partial \nu} \left(\sin \nu \frac{\partial \xi}{\partial \nu} \right) + \frac{\partial}{\partial \phi} \left(\frac{1}{\sin \nu} \frac{\partial \xi}{\partial \phi} \right) \right] + \frac{\bar{\epsilon}}{4} \hbar \Omega_0 \cos^2 \nu \xi^* \xi + \frac{\bar{g}_{2D}}{2} \xi^{*2} \xi^2 \right\}, \quad (51)$$

where $\bar{g}_{2D} = \left(\frac{m\Omega_0}{2\pi\hbar} \right)^{1/2} \bar{g}_{\text{int}} = \left(\frac{m\Omega_0\Lambda}{2\pi\hbar} \right)^{1/2} g_{\text{int}}$. With this we conclude that (51) is the appropriate Hamiltonian in the thin-shell limit apart from the diverging additive constant $E_2 + E_0^{(1)} + E_0^{(0)} + C_0$.

5. Particular cases

By taking the functional derivative of (51), it is possible to obtain the wavefunction that minimizes it with the corresponding Lagrange multiplier μ and with the constraint (45) as follows

$$\frac{\delta H_{\text{eff}}}{\delta \xi^*(x^i)} - \mu \frac{\delta N}{\delta \xi^*(x^i)} = 0, \quad (52)$$

which straightforwardly leads to

$$-\frac{\hbar^2}{2mA^2 \sin \nu} \left[\frac{\partial}{\partial \nu} \left(\sin \nu \frac{\partial \xi}{\partial \nu} \right) + \frac{\partial}{\partial \phi} \left(\frac{1}{\sin \nu} \frac{\partial \xi}{\partial \phi} \right) \right] + \frac{\bar{\epsilon}}{4} \hbar \Omega_0 \cos^2 \nu \xi + \bar{g}_{2D} \xi^* \xi^2 = \mu \xi. \quad (53)$$

Now let us consider some particular cases for this 2D time-independent GPE.

5.1. Spherical shell

Considering the particular situation of the spherical shell, i.e. $\bar{\epsilon} = 0$, there are some possible simplifications in the Hamiltonian. The wavefunction corresponding to the lowest energy state $\xi(x^i)$ is a constant along the shell since the BEC particles are uniformly distributed around the bubble.

Let us begin by finding the constant value of ξ through (45) for the ground state of the system

$$\xi = \sqrt{\frac{N}{A^2 4\pi}}. \quad (54)$$

Substituting this value for our wavefunction into (51) we find with $\bar{\epsilon} = 0$ the corresponding energy

$$E_S = \frac{\bar{g}_{2D}}{8A^2\pi} N^2. \quad (55)$$

This is the Λ^0 contribution to the energy for the spherical shell. Thus, the total ground-state energy in this case is $E_2 + E_0^{(1)} + E_0^{(0)} + C_0 + E_S$.

5.2. Thomas-Fermi approximation

For situations where the interaction energy is much larger than the kinetic energy the so-called Thomas-Fermi approximation can be applied. For the Hamiltonian 51 this corresponds for example to the situation where $N \Rightarrow \infty$ or $A \Rightarrow \infty$.

In order to calculate the wavefunction $\xi(x^i)$, we take (53) without the kinetic energy term, as follows

$$\xi = \sqrt{\frac{\mu - \frac{\bar{\epsilon}}{4}\hbar\Omega_0 \cos^2 \nu}{\bar{g}_{2D}}}. \quad (56)$$

As expected, $\xi(x^i)$ has an angular dependence along the shell. Inserting it in equation (51) and solving, we find the Thomas-Fermi energy

$$E_{\text{TF}} = \frac{\pi A^2 (80\mu^2 - \bar{\epsilon}^2 \hbar^2 \Omega_0^2)}{40\bar{g}_{2D}}, \quad (57)$$

which is the ground state Λ^0 energy contribution without the additive constants. Taking into account (45) it can be rewritten in terms of the total number of particles N as

$$E_{\text{TF}} = \frac{\pi A^2}{40\bar{g}_{2D}} \left(\frac{5\bar{g}_{2D}^2 N^2}{\pi^2 A^4} + \frac{10}{3\pi A^2} \bar{g}_{2D} N \bar{\epsilon} \hbar \Omega_0 - \frac{4\bar{\epsilon}^2 \hbar^2 \Omega_0^2}{9} \right). \quad (58)$$

Thus, the total ground-state energy in this case is $E_2 + E_0^{(1)} + E_0^{(0)} + C_0 + E_{\text{TF}}$.

6. Perturbative solutions

Although the main result of our work is the step-by-step construction of the theory for BECs in the thin-shell limit, this paper also provides solutions to particular cases of the spherical shell and the Thomas-Fermi regime for our effective Hamiltonian showing the mathematical aspects of the correspondent wavefunctions. Now, in this chapter, we perturbatively solve the system with respect to the geometrical distortion $\bar{\epsilon}$ in order to find both the ground-state wavefunction and the excitations frequencies.

6.1. Perturbative ground state

Let us perturbatively solve 53 which we rewrite as

$$\frac{1}{2mA^2}\hat{L}^2\xi + \lambda \cos^2(\nu)\xi + \bar{g}_{2D}|\xi|^2\xi = \mu\xi, \quad (59)$$

where $\lambda = \bar{\epsilon}\hbar\Omega_0/4$ and $\int dS |\xi|^2 = A^2 \int_0^{2\pi} d\phi \int_0^\pi d\nu \sin\nu |\xi|^2 = N$.

The usual angular momentum operator \hat{L}^2 has eigenvalues $\hbar^2 l(l+1)$ and normalized eigenfunctions given by the spherical harmonics $Y_l^m(\nu, \phi)$.

Since the set $\{Y_l^m\}$ is a complete orthogonal basis over the spherical domain, ξ can be expanded in such a basis. However since here we are looking for the unique lowest energy state which is represented by a ϕ -independent real function $\xi(\nu)$, then its expansion becomes

$$\xi(\nu) = \frac{\sqrt{N}}{A} \sum_i c_i Y_i^0(\nu), \quad (60)$$

so that $\sum_i |c_i|^2 = 1$.

Here one important property of Y_l^m is $\cos(\nu)Y_l^m = \alpha_l^m Y_{l-1}^m + \alpha_{l+1}^m Y_{l+1}^m$, where $\alpha_l^m = \sqrt{\frac{(l-m)(l+m)}{(2l-1)(2l+1)}}$ and therefore

$$\cos^2(\nu)Y_l^m = \alpha_l^m \alpha_{l-1}^m Y_{l-2}^m + \left[(\alpha_l^m)^2 + (\alpha_{l+1}^m)^2 \right] Y_l^m + \alpha_{l+2}^m \alpha_{l+1}^m Y_{l+2}^m. \quad (61)$$

Using these properties in (59) leads to

$$\varepsilon_i c_i + \lambda \sum_j M_{ij} c_j + 4\pi g_{\text{eff}} \sum_{jkl} \Gamma_{ijkl} c_j c_k c_l = \mu c_i, \quad (62)$$

where we define the effective interaction strength $g_{\text{eff}} = (\bar{g}_{2D}N)/(4\pi A^2)$ and

$$\varepsilon_l = \frac{\hbar^2 l(l+1)}{2mA^2}, \quad (63)$$

$$M_{ij} = 2\pi \int_0^\pi d\nu \sin(\nu) Y_i^0(\nu) Y_j^0(\nu) \cos^2(\nu), \quad (64)$$

$$\Gamma_{ijkl} = 2\pi \int_0^\pi d\nu \sin(\nu) Y_i^0(\nu) Y_j^0(\nu) Y_k^0(\nu) Y_l^0(\nu), \quad (65)$$

which have the specific values

$$\Gamma_{ij00} = \frac{1}{4\pi} \delta_{ij}, \quad M_{i0} = \frac{1}{3} \delta_{i0} + \frac{2}{3\sqrt{5}} \delta_{i,2}, \quad (66)$$

where δ_{ij} is the Kroenecker delta.

Now we apply a generalization of Rayleigh-Schrödinger perturbation theory in order to solve the nonlinear equation (62), i.e.,

$$c_i = c_i^{(0)} + \lambda c_i^{(1)} + \lambda^2 c_i^{(2)} + \dots, \quad \text{and} \quad \mu = \mu^{(0)} + \lambda \mu^{(1)} + \lambda^2 \mu^{(2)} + \dots \quad (67)$$

Considering the zeroth-order solution, we find $c_i^{(0)} = \delta_{i,0}$ and $\mu^{(0)} = g_{\text{eff}}$.

In order to use the same normalization as in Rayleigh-Schrödinger perturbation theory, we define the renormalization constant Z according to

$$a_i = Z c_i, \quad (68)$$

and therefore

$$|Z|^2 = \sum_i |a_i|^2. \quad (69)$$

The new coefficients can now be normalized as $\sum_i a_i c_i^{(0)} = a_0 = 1$.

Equation (62) then becomes

$$\varepsilon_i a_i + \lambda \sum_j M_{ij} a_j + \frac{4\pi g_{\text{eff}}}{|Z|^2} \sum_{jkl} \Gamma_{ijkl} a_j a_k a_l = \mu a_i, \quad (70)$$

with the expansion

$$a_i = a_i^{(0)} + \lambda a_i^{(1)} + \lambda^2 a_i^{(2)} + \dots \quad (71)$$

where $a_i^{(l)}$ are $|Z|^2$ dependent, i.e., we treat $|Z|^2$ as another constant and expand the results according to (68) and (69) at the end. In addition, since $a_0 = 1$, then

$$a_0^{(n)} = 0, \quad n > 0, \quad (72)$$

which implies that $|Z|^2 = 1 + O(\lambda^2)$ and could be considered equal to 1 if one is interested only in first-order perturbation theory.

Substituting (71) into (70) and applying (66), we get

$$\begin{aligned} \varepsilon_i a_i^{(n)} + \sum_j M_{ij} a_j^{(n-1)} + 3 \frac{g_{\text{eff}}}{|Z|^2} a_i^{(n)} + \frac{4\pi g_{\text{eff}}}{|Z|^2} \sum_{\substack{j,k,l \\ r,s,t < n}} \Gamma_{ijkl} a_j^{(r)} a_k^{(s)} a_l^{(t)} \delta_{r+s+t,n} \\ = \mu^{(0)} a_i^{(n)} + \sum_{m=1}^n \mu^{(m)} a_i^{(n-m)}. \end{aligned} \quad (73)$$

Considering $i = 0$ in (73), we get the recursion relation for $\mu^{(n)}$

$$\mu^{(n)} = \sum_j M_{0j} a_j^{(n-1)} + \frac{4\pi g_{\text{eff}}}{|Z|^2} \sum_{\substack{j,k,l \\ r,s,t < n}} \Gamma_{0jkl} a_j^{(r)} a_k^{(s)} a_l^{(t)} \delta_{r+s+t,n}, \quad (74)$$

while for $i > 0$ in (73), we get the recursion relation for $a_i^{(n)}$

$$\begin{aligned} a_i^{(n)} = \frac{1}{\varepsilon_i - \mu_0 + \frac{3g_{\text{eff}}}{|Z|^2}} \left[- \sum_j M_{ij} a_j^{(n-1)} \right. \\ \left. - \frac{g_{\text{eff}}}{|Z|^2} \sum_{\substack{j,k,l \\ r,s,t < n}} \Gamma_{ijkl} a_j^{(r)} a_k^{(s)} a_l^{(t)} \delta_{r+s+t,n} + \sum_{m=1}^n \mu^{(m)} a_i^{(n-m)} \right]. \end{aligned} \quad (75)$$

Note that in the linear case where $g_{\text{eff}} = 0$, Eqs. (74) and (75) reduce to usual Rayleigh-Schrödinger recursion formulae where no reference to the normalization constant Z is necessary.

Now, direct substitution for $i > 0$ gives

$$\mu^{(1)} = M_{00} = \frac{1}{3}, \quad (76)$$

$$a_i^{(1)} = -\frac{1}{\varepsilon_i - \mu_0 + \frac{3g_{\text{eff}}}{|Z|^2}} M_{i0} = -\frac{1}{\varepsilon_2 + \frac{(3-|Z|^2)g_{\text{eff}}}{|Z|^2}} \frac{2}{3\sqrt{5}} \delta_{i2}. \quad (77)$$

Since $|Z|^2 = 1 + O(\lambda^2)$, from (68) we have

$$c_i = \delta_{i0} - \lambda \frac{1}{\varepsilon_2 + 2g_{\text{eff}}} \frac{2}{3\sqrt{5}} \delta_{i2} + O(\lambda^2), \quad (78)$$

which according to (60) gives the ground state wave function

$$\xi_0(\nu) = \sqrt{\frac{N}{4\pi A^2}} \left[1 - \lambda \frac{1}{\varepsilon_2 + 2g_{\text{eff}}} \left(\cos^2 \nu - \frac{1}{3} \right) \right] + O(\lambda^2). \quad (79)$$

6.2. Perturbative excitation spectrum

We consider now the dynamics of small excitations over the ground state $\xi^{(0)}$ which are given by the time-dependent GP equation

$$\frac{1}{2mA^2} \hat{L}^2 \xi + \lambda \cos^2(\nu) \xi + \bar{g}_{2D} |\xi|^2 \xi = i\hbar \frac{\partial \xi}{\partial t}, \quad (80)$$

where $\xi(t) = e^{-i\mu t/\hbar}(\xi_0 + \delta\xi(t))$ and $\delta\xi(t) = ue^{-i\omega t} - v^*e^{i\omega t}$ represent small corrections, yielding the Bogouliubov equations [58]

$$TU = \hbar\omega \sigma U, \quad (81)$$

with

$$T = \begin{pmatrix} \frac{1}{2mA^2} \hat{L}^2 + \lambda \cos^2(\nu) + 2\bar{g}_{2D} |\xi_0|^2 - \mu & -\bar{g}_{2D} |\xi_0|^2 \\ -\bar{g}_{2D} |\xi_0|^2 & \frac{1}{2mA^2} \hat{L}^2 + \lambda \cos^2(\nu) + 2\bar{g}_{2D} |\xi_0|^2 - \mu \end{pmatrix}, \quad (82)$$

$$\sigma = \begin{pmatrix} 1 & 0 \\ 0 & -1 \end{pmatrix}, \quad (83)$$

$$U = \begin{pmatrix} u \\ v \end{pmatrix}. \quad (84)$$

According to [59,60], we can apply Rayleigh-Schrödinger perturbation theory to the generalized eigenvalue problem (81), by choosing the appropriate “scalar product”

$$(U', U) = \int dS U^\dagger(\nu, \phi) \sigma U(\nu, \phi), \quad (85)$$

where U^\dagger is the hermitian conjugate of the vector U and dS stands for the surface element in the spherical coordinates (ν, ϕ) .

In order to proceed, we must expand (82) in power series of λ

$$T = T_0 + \lambda T_1 + O(\lambda^2). \quad (86)$$

From (79) and (76), we have

$$T_0 = \begin{pmatrix} \frac{1}{2mA^2} \hat{L}^2 + \frac{\bar{g}_{2D}N}{4\pi A^2} & -\frac{\bar{g}_{2D}N}{4\pi A^2} \\ -\frac{\bar{g}_{2D}N}{4\pi A^2} & \frac{1}{2mA^2} \hat{L}^2 + \frac{\bar{g}_{2D}N}{4\pi A^2} \end{pmatrix}, \quad (87)$$

$$T_1 = \begin{pmatrix} 1 - 4\frac{\bar{g}_{2D}N}{4\pi A^2} \frac{1}{\frac{3\hbar^2}{mA^2} + \frac{\bar{g}_{2D}N}{2\pi A^2}} & \left(\cos^2 \nu - \frac{1}{3}\right) \begin{pmatrix} 1 & 0 \\ 0 & 1 \end{pmatrix} \\ + 2\frac{\bar{g}_{2D}N}{4\pi A^2} \frac{1}{\frac{3\hbar^2}{mA^2} + \frac{\bar{g}_{2D}N}{2\pi A^2}} \left(\cos^2 \nu - \frac{1}{3}\right) \begin{pmatrix} 0 & 1 \\ 1 & 0 \end{pmatrix} \end{pmatrix}. \quad (88)$$

These equations can now be written in the basis $\{Y_l^m\}$, i.e.,

$$U(\nu, \phi) = A^{-1} \sum_{lm} c_{(l,m)} Y_l^m(\nu, \phi), \quad (89)$$

so that the normalization condition in terms of the vectors $\{c_{(l,m)}\}$ is

$$(U', U) = \sum_{lm} c_{(l,m)}^\dagger \sigma c_{(l,m)} = 1 \quad (90)$$

Also we have for T_0 :

$$T_0^{(l,m),(l',m')} = \begin{pmatrix} \varepsilon_l + g_{\text{eff}} & -g_{\text{eff}} \\ -g_{\text{eff}} & \varepsilon_l + g_{\text{eff}} \end{pmatrix} \delta_{l,l'} \delta_{m,m'}, \quad (91)$$

while (61) gives

$$\begin{aligned} T_1^{(l,m),(l',m')} &= \left(1 - 4g_{\text{eff}} \frac{1}{\varepsilon_2 + 2g_{\text{eff}}}\right) \times \begin{pmatrix} 1 & 0 \\ 0 & 1 \end{pmatrix} \\ &\times \left(\alpha_l^m \alpha_{l-1}^m \delta_{l,l'-2} + \left[(\alpha_l^m)^2 + (\alpha_{l+1}^m)^2\right] \delta_{l,l'} + \alpha_{l+2}^m \alpha_{l+1}^m \delta_{l,l'+2} - \frac{1}{3} \delta_{l,l'}\right) \delta_{m,m'} \\ &+ 2g_{\text{eff}} \frac{1}{\varepsilon_2 + 2g_{\text{eff}}} \times \begin{pmatrix} 0 & 1 \\ 1 & 0 \end{pmatrix} \\ &\times \left(\alpha_l^m \alpha_{l-1}^m \delta_{l,l'-2} + \left[(\alpha_l^m)^2 + (\alpha_{l+1}^m)^2\right] \delta_{l,l'} + \alpha_{l+2}^m \alpha_{l+1}^m \delta_{l,l'+2} - \frac{1}{3} \delta_{l,l'}\right) \delta_{m,m'}. \end{aligned} \quad (92)$$

Direct diagonalization of (91) gives the eigenvalues for each (l', m')

$$\hbar \left(\omega_{\pm}^{(l',m')}\right)_0 = \pm \sqrt{\varepsilon_{l'}(\varepsilon_{l'} + 2g_{\text{eff}})}, \quad (93)$$

with the corresponding eigenvectors

$$\left(c_{(l,m)}^{(l',m')}\right)_0 = \left(C_{(l,m)}^{(l',m')}\right)^{-1/2} \begin{pmatrix} \frac{g + \varepsilon_l \pm \sqrt{\varepsilon_l(\varepsilon_l + 2g_{\text{eff}})}}{g} \\ 1 \end{pmatrix} \delta_{l,l'} \delta_{m,m'} + O(\lambda), \quad (94)$$

where $C_{(l,m)}^{(l',m')}$ ensures the normalization $(U_{\pm}^{(0)}, U_{\pm}^{(0)}) = 1$.

The first-order correction to the eigenvalues $\hbar\omega_{\pm}^{(l',m')}$ will be given by the usual Rayleigh-Schrödinger theory according to our generalized “scalar product”

$$\hbar\left(\omega_{\pm}^{(l',m')}\right)_1 = (U_{\pm}^{(0)}, T_1 U_{\pm}^{(0)}), \quad (95)$$

which in the basis of $\{Y_l^m\}$ becomes

$$\hbar\left(\omega_{\pm}^{(l',m')}\right)_1 = \sum_{(l,m),(l',m')} \left(c_{(l,m)}^{(l',m')}\right)_0^{\dagger} \sigma T_1^{(l,m),(l',m')} \left(c_{(l,m)}^{(l',m')}\right)_0. \quad (96)$$

Using (92), we have

$$\hbar\left(\omega_{\pm}^{(l',m')}\right)_1 = \left(1 - 4g_{\text{eff}} \frac{1}{\varepsilon_2 + 2g_{\text{eff}}}\right) \left[\left(\alpha_{l'}^{m'}\right)^2 + \left(\alpha_{l'+1}^{m'}\right)^2 - \frac{1}{3}\right]. \quad (97)$$

With this, we finally have the final expression for excitation frequencies

$$\begin{aligned} \omega_{\pm}^{(l,m)} = & \pm \sqrt{\frac{l(l+1)}{2mA^2} \left[\frac{\hbar^2 l(l+1)}{2mA^2} + \frac{\bar{g}_{2D} N}{2\pi A^2} \right] + \frac{\bar{\epsilon}\Omega_0}{4} \left(1 - \frac{2}{\frac{6\pi\hbar^2}{\bar{g}_{2D} m N} + 1} \right)} \\ & \left[\frac{(l-m)(l+m)}{(2l-1)(2l+1)} + \frac{(l-m+1)(l+m+1)}{(2l+1)(2l+3)} - \frac{1}{3} \right] + O(\bar{\epsilon}^2). \end{aligned} \quad (98)$$

7. Summary and conclusions

In this paper, we have shown how the parameters of a bubble trap have to be carefully chosen in order to allow the existence of a thin-shell limit. Under the adequate assumptions, we were able to perform a dimensional compactification which leads to an effective 2D Hamiltonian for interacting BECs. From the experimental point of view, we demonstrated that, in order to avoid the collapse of the condensate, the thin-shell limit must be taken in such way that the spatial distortion caused by the eccentricity of the surface must be kept in the same order of magnitude as the width of the Gaussian distribution perpendicular to the surface. Details on how our experimentally obtained bubble-trap potentials fit into our general theory were also provided. In addition, applications of this theory to stationary systems as well as the excitation frequencies were calculated.

8. Acknowledgments

This work was supported by CNPq (Conselho Nacional de Desenvolvimento Científico e Tecnológico), and DAAD-CAPES PROBRAL, Brazil Grant number 88887.627948/2021-00.

Appendix A. Derivation of constants in H_0

It is necessary to specify some constants inside the Hamiltonian H_0 . In order to do that, let us use the formula for the derivatives of the determinant of a quantity B

$$\begin{cases} \frac{d|B|}{d\lambda} = |B| \text{Tr}(B^{-1} \frac{dB}{d\lambda}), \\ \frac{d^2|B|}{d\lambda^2} = |B| \text{Tr}(B^{-1} \frac{dB}{d\lambda})^2 + |B| \text{Tr}(B^{-1} \frac{d^2B}{d\lambda^2}) - |B| \text{Tr}(B^{-1} \frac{dB}{d\lambda} B^{-1} \frac{dB}{d\lambda}). \end{cases} \quad (\text{A.1})$$

The metric g with the Taylor series up to second order is

$$g(s, \epsilon) = g_0 + g_1 \Lambda^{-1/2} y + g_\epsilon \Lambda^{-1} \bar{\epsilon} + \frac{1}{2} g_2 \Lambda^{-1} y^2 + O(\Lambda^{-3/2}), \quad (\text{A.2})$$

with $g(0, 0) = g_0$, $\frac{\partial g(0,0)}{\partial s} = g_1$, $\frac{\partial g(0,0)}{\partial \epsilon} = g_\epsilon$, and $\frac{\partial^2 g(0,0)}{\partial s^2} = g_2$. With this our γ derivatives can be expressed as $\gamma_1 = \text{Tr}(g_0^{-1} g_1)$ and $\gamma_2 = \text{Tr}(g_0^{-1} g_1)^2 + \text{Tr}(g_0^{-1} g_2) - \text{Tr}(g_0^{-1} g_1 g_0^{-1} g_1)$.

In the thin-shell limit the metric becomes the spherical one giving

$$g_0 = \begin{pmatrix} 1 & 0 & 0 \\ 0 & A^2 & 0 \\ 0 & 0 & A^2 \sin^2 \nu \end{pmatrix}, g_1 = \begin{pmatrix} 0 & 0 & 0 \\ 0 & 2A & 0 \\ 0 & 0 & 2A \sin^2 \nu \end{pmatrix}, g_2 = \begin{pmatrix} 0 & 0 & 0 \\ 0 & 2 & 0 \\ 0 & 0 & 2 \sin^2 \nu \end{pmatrix}. \quad (\text{A.3})$$

that can be used to calculate the traces granting $\gamma_1 = \frac{4}{A}$ and $\gamma_2 = \frac{12}{A^2}$.

- [1] Anderson M H, Ensher J R, Matthews M R, Wieman C E and Cornell E A 1995 Observation of Bose-Einstein condensation in a dilute atomic vapor *Science* 269, 5221
- [2] Davis K B, Mewes M O, Andrews M R, van Druten N J, Durfee D S, Kurn D M and Ketterle W 1995 Bose-Einstein condensation in a gas of sodium atoms *Phys. Rev. Lett.* 75, 22
- [3] Zobay O and Garraway B M 2000 Properties of coherent matter-wave bubbles *acta physica slovacica* 50, 3
- [4] Zobay O and Garraway B M 2001 Two-dimensional atom trapping in field-induced adiabatic potentials *Phys. Rev. Lett.* 86, 7
- [5] Zobay O and Garraway B M 2004 Atom trapping and two-dimensional Bose-Einstein condensates in field-induced adiabatic potentials *Phys. Rev. A* 69, 2
- [6] Colombe Y, Knyazchyan E, Morizot O, Mercier B, Lorent V and Perrin H 2004 Ultracold atoms confined in rf-induced two-dimensional trapping potentials *Europhys. Lett.* 67, 4
- [7] Garraway B and Perrin H 2016 Recent developments in trapping and manipulation of atoms with adiabatic potentials *J. Phys. B* 49, 17
- [8] Perrin H and Garraway B M 2017 Trapping atoms with radio frequency adiabatic potentials *At. Mol. Opt. Phys.* 66
- [9] White M, Gao H, Pasienski M, and DeMarco B 2006 Bose-Einstein condensates in rf-dressed adiabatic potentials *Phys. Rev. A* 74, 2
- [10] Merloti K, Dubessy R, Longchambon L, Perrin A, Pottier P E, Lorent V and Perrin H 2013 A two-dimensional quantum gas in a magnetic trap *New Journal of Physics* 15
- [11] van Zoest T et al 2010 Bose-Einstein condensation in microgravity *Science* 328, 5985
- [12] Condon G, Rabault M, Barrett B, Chichet L, Arguel, Eneriz-Imaz H, Naik D, Bertoldi A, Battelier B, Bouyer P, and Landragin A 2019 All-optical Bose-Einstein condensates in microgravity *Phys. Rev. Lett.* 123, 24
- [13] Elliott E R, Krutzik M C, Williams J R, Thompson J R, and Aveline D C 2018 NASA's Cold Atom Lab (CAL): system development and ground test status *npj Microgravity* 4, 1
- [14] Aveline D C, Williams J R, Elliott E R, Dutenhoffer C, Kellogg J R, Kohel J M, Lay N E, Oudrhiri K, Shotwell R F, Yu N and Thompson R J 2020 Observation of Bose-Einstein condensates in an Earth-orbiting research lab *Nature* 582, 7811
- [15] Becker D, et al. 2018 Space-borne Bose-Einstein condensation for precision interferometry *Nature* 562, 7727
- [16] Lundblad N 2017 Microgravity dynamics of bubble-geometry Bose-Einstein condensates (https://taskbook.nasaprs.com/Publication/index.cfm?action=public_query_taskbook_content&TASKID=11095)
- [17] Lundblad N, Carollo R A, Lannert C, Gold M J, Jiang X, Paseltiner D, Sergay N and Aveline D C 2019 Shell potentials for microgravity Bose-Einstein condensates *Microgravity* 5,1
- [18] Frye K et al 2021 The Bose-Einstein condensate and cold atom laboratory *EPJ Quantum Technol.* 8, 1
- [19] Carollo R A, Aveline D C, Rhyno B, Vishveshwara S, Lannert C, Murphree J D, Elliott E R, Williams J R, Thompson R J and Lundblad N 2022 Observation of ultracold atomic bubbles in orbital microgravity *Nature* 606, 7913
- [20] Cho A 2017 Trapped in orbit *Science* 357, 3
- [21] Guo Y, Gutierrez E M, Rey D, Badr T, Perrin A, Longchambon L, Bagnato V, Perrin H, and Dubessy R 2021 An annular quantum gas induced by dimensional reduction on a shell *arXiv:2105.12981*
- [22] Shibata K, Ikeda H, Suzuki R, and Hirano T 2020 Compensation of gravity on cold atoms by a linear optical potential *Phys. Rev. Res.* 2, 1
- [23] Wolf A, Boegel P, Meister M, BalaÅŸ A, Gaaloul N, and Efremov M A 2022 Shell-shaped Bose-Einstein condensates based on dual-species mixtures *Phys. Rev. A* 106, 013309
- [24] Jia F, Huang Z, Qiu L, Zhou R, Yan Y, and Wang D, 2020 Expansion dynamics of a shell-shaped Bose-Einstein condensate *arXiv:2208.01360*

- Expansion dynamics of a shell-shaped Bose-Einstein condensate, arXiv:2208.01360
- [25] Lannert C, Wei T C and Vishveshwara S 2007 Dynamics of condensate shells: collective modes and expansion *Phys. Rev. A* 75, 1
 - [26] Prestipino S and Giaquinta P V 2019 Ground state of weakly repulsive soft-core bosons on a sphere *Phys. Rev. A* 99, 6
 - [27] Bereta S J, Madeira L, Caracanhas M A and Bagnato V S 2019 Bose-Einstein condensation in spherically symmetric traps *Am. J. Phys.* 87, 11
 - [28] Tononi A and Salasnich L 2019 Bose-Einstein condensation on the surface of a sphere *Phys. Rev. Lett.* 123, 16
 - [29] Tononi A, Cinti F and Salasnich L 2020 Quantum bubbles in microgravity *Phys. Rev. Lett.* 125, 1
 - [30] Sun K, Padavic K, Yang F, Vishveshwara S and Lannert C 2018 Static and dynamic properties of shell-shaped condensates *Phys. Rev. A* 98, 1
 - [31] Padavić K, Sun K, Lannert C and Vishveshwara S 2018 Physics of hollow Bose-Einstein condensates *Europhys. Lett.* 120, 2
 - [32] de Castro Diniz P, Oliveira E A B, Lima A R P and de Lima Henn E A 2020 Ground state and collective excitations of a dipolar Bose-Einstein condensate in a bubble trap *Scientific Reports* 10, 1
 - [33] Zhang J and Ho T L 2018 Potential scattering on a spherical surface *Journal of Physics B: Atomic, Molecular and Optical Physics* 51, 11
 - [34] Mitra K, Williams C J, and Sa de Melo C A R 2008 Superfluid and Mott-insulating shells of bosons in harmonically conned optical lattices *Phys. Rev. A* 77, 3
 - [35] Tononi A, Pelster A, and Salasnich L 2022 Topological superfluid transition in bubble-trapped condensates *Phys. Rev. Research* 4, 1
 - [36] Pará Y, Palumbo G, Macri T 2021 Probing non-Hermitian phase transitions in curved space via quench dynamics *Phys. Rev. B* 103, 15
 - [37] Caracanhas M A, Massignan P, and Fetter A L 2022 Superfluid vortex dynamics on an ellipsoid and other surfaces of revolution *Phys. Rev. A* 105, 2
 - [38] Bereta S J, Caracanhas M A, and Fetter A L 2021 Superfluid vortex dynamics on a spherical film *Phys. Rev. A* 103, 5
 - [39] Dritschel D G and Boatto S 2015 The motion of point vortices on closed surfaces *Proc. R. Soc. A.* 471, 20140890
 - [40] Hally D 1980 Stability of streets of vortices on surfaces of revolution with a reflection symmetry *J. Math. Phys.* 21, 1
 - [41] Castilho C and Machado H 2008 The N-vortex problem on asymmetric ellipsoid: A perturbation approach *J. Math. Phys.* 49, 2
 - [42] Rodrigues A R, Castilho C, and Koiller J 2018 Vortex pairs on a triaxial ellipsoid and Kimura's conjecture *J. Geom. Mech.* 10, 2
 - [43] Turner A M, Vitelli V, and Nelson D R 2010 Vortices on curved surfaces *Rev. Mod. Phys.* 82, 2
 - [44] Padavić K, Sun K, Lannert C, and Vishveshwara S 2020 Vortex-antivortex physics in shell shaped Bose-Einstein condensates *Phys. Rev. A* 102, 4
 - [45] Kühnel W 2002 *Differential geometry: curves-surfaces-manifolds* 2nd edn (Providence, R.I.: American Mathematical Society)
 - [46] Lee J M 2000 *Introduction to topological manifolds* (Springer-Verlag)
 - [47] Lee J M 2009 *Manifolds and differential geometry, graduate studies in mathematics* (Providence: American Mathematical Society)
 - [48] Weisstein E W Smooth manifold (<https://mathworld.wolfram.com/SmoothManifold.html>)
 - [49] Whitney H 1936 Differentiable manifolds *Annals of mathematics* 37, 3
 - [50] Smoller J and Temple B 1994 Shock-wave solutions of the Einstein equations: the Oppenheimer-Snyder model of gravitational collapse extended to the case of non-zero pressure *Arch. Ration. Mech. Anal.* 128, 3

- [51] Iofa M Z 2016 Kodama-Schwarzschild versus Gaussian normal coordinates picture of thin-shells *Adv. High Energy Phys.* 2016, 5632734
- [52] Moller N S, dos Santos F E A, Bagnato V S, and Pelster A 2020 Bose-Einstein condensation on curved manifolds *New J. Phys.* 22, 6
- [53] Moon P H and Spencer D E 1988 *Field theory handbook: including coordinate systems, differential equations, and their solutions* 2nd edn (New York: Springer Verlag)
- [54] Morse P M and Feshbach H 1953 *Methods of Theoretical Physics, Part I* (New York: McGraw-Hill)
- [55] Vaughn M T 2007 *Introduction to mathematical physics* (Weinheim: Wiley-VCH Verlag GmbH & Co.)
- [56] Butkov E 1968 *Mathematical Physics* (Reading, Mass: Addison-Wesley Pub. Co)
- [57] Griffiths D 2004 *Introduction to Quantum Mechanics* 2nd edn (Prentice Hall)
- [58] Pethick C J and Smith H 2008 *Bose-Einstein Condensation in Dilute Gases* (Cambridge University Press)
- [59] Peters G and Wilkinson J H 1970 $Ax = \lambda Bx$ and the generalized eigenproblem *SIAM Journal on Numerical Analysis* 7, 4
- [60] Bender C M 2007 Making sense of non-Hermitian Hamiltonians *Rep. Prog. Phys.* 70, 6